# Understanding Zinc-containing Species in BOS Dust

*R.J. Longbottom[1], D.J. Pinson[2,5], S.J. Chew[3,5] and B.J. Monaghan[4,5]*

1. Research Fellow, Faculty of Engineering and Information Science, University of Wollongong, Wollongong NSW 2522. Email: rayl@uow.edu.au
2. Senior Technology and Development Engineer, BlueScope Coke and Ironmaking Technology, Port Kembla NSW 2505. Email: david.pinson@bluescopesteel.com
3. Principal Technology and Development Engineer, BlueScope Coke and Ironmaking Technology, Port Kembla NSW 2505. Email: sheng.chew@bluescopesteel.com
4. Professor, Faculty of Engineering and Information Science, University of Wollongong, Wollongong NSW 2522, Email: monaghan@uow.edu.au
5. ARC Research Hub for Australian Steel Innovation, Wollongong NSW 2522.

Keywords: BOS dust, steel plant by-products, recycling, zinc, zinc ferrite

## ABSTRACT

Recycling steel plant by-products is a critical issue for achieving both environmental and economic sustainability of integrated steel plants. A key steel plant by-product stream is dust from basic oxygen steelmaking (BOS), which can be recycled back to the BOS vessel as iron units and to aid slag formation. The major limitations for its recycling are zinc and the uncertainty in zinc speciation of the dust. This uncertainty affects the amount of dust recycled and how it interacts with the slag during processing. BOS dust in stockpiles can undergo self-sintering reactions that oxidise the iron-bearing components. As this occurs, zinc (or oxide) may combine with iron oxides to form a zinc-iron spinel solid solution phase. Knowing which zinc-bearing species are present in the BOS dust is a key aspect in understanding and developing an efficient recycling process for the dust.

To overcome difficulties associated with phase identification in the BOS dust (both fresh and self-sintered), particularly the magnetite-zinc ferrite spinel solid solution using XRD/SEM/EDS, high end characterisation tools, TEM and Mössbauer spectroscopy, were also used. Such an approach allowed improved phase identification of key zinc- and iron-bearing phases that were not previously resolvable.

The zinc in fresh BOS dust was mostly present as extremely fine separate particles of zinc oxide, attached to the iron particles. These extremely fine particles were < 10 nm in size. Additionally, a small amount of zinc ferrite was also identified within the sample (most likely contained within a magnetite-zinc ferrite spinel solid solution).

However, the zinc in the self-sintered BOS dust, was found to be present entirely in a magnetite-zinc ferrite spinel solid solution. While this spinel phase had been previously identified by XRD, it was not clear that it contained zinc. The Mössbauer results provided definitive evidence of zinc within the spinel phase.

## INTRODUCTION

On-plant recycling of steel plant by-products will help achieve the environmental and economic sustainability of integrated steel plants, reducing emissions by replacing raw materials and recovering the valuable components within the by-products (Nyirenda, 1991, Ahmed *et al*. 2015). One key by-product in an integrated steel plant is dust from the basic oxygen steelmaking (BOS) process. When oxygen is blown at supersonic velocity to decarburise steel, significant amounts of dust are generated. This dust is made up of very fine particles of steel and slag droplets, as well as flux fines. When the dust is recycled back to the BOS, these slag droplets and flux fines have value and aid slag formation (Longbottom *et al*. 2019a, 2019b).

Unfortunately, there are limitations on the recycling of BOS dust, primarily Zn and the uncertainty in Zn speciation of the dust. (Stewart and Barron, 2020, Longbottom *et al*. 2020). Which Zn-bearing phases are present in the BOS dust strongly affects how the BOS dust interacts with the slag during processing. As such, the uncertainty in the Zn speciation in the dust affects the amount that can be recycled to the BOS. Hence, it is important to understand what Zn-bearing phases are present in the BOS dust, whether as metallic Zn, ZnO or in a complex zinc ferrite-magnetite ($ZnFe_2O_4$-$Fe_3O_4$) spinel solid solution.

Zn in the BOS dust results from the high temperatures (>> 1600°C) in the BOS process causing volatilisation of Zn (and other tramp elements) to the gas phase (Nedar, 1996). As the gas phase is cooled in the extraction process, the volatilised Zn can condense as separate particles or onto existing dust particles.

BOS dust is often removed from the off-gas using a wet scrubbing process, resulting in a slurry that is usually dewatered to produce a low moisture filter cake that is stockpiled for future recycling. When stored in stockpiles prior to recycling, BlueScope BOS dust has been found to self-sinter (Longbottom 2019a, 2019b, 2020). Using TGA-DSC and *in situ* X-ray diffraction (XRD) techniques, the self-sintered dust has been shown to have undergone exothermic oxidation reactions in the stockpiles (Longbottom *et al.* 2019a, 2019b, 2020). As part of these oxidation reactions, ZnO reacted with iron oxides to form the $ZnFe_2O_4$-$Fe_3O_4$ spinel solid solution. The formation of the $ZnFe_2O_4$ side of the solid solution is shown in reaction (1).

$$ZnO_{(s)} + Fe_2O_{3(s)} = ZnFe_2O_{4(s)} \quad (1)$$

However, these studies also highlighted a number of issues in the characterisation of the Zn bearing phases. Using scanning electron microscopy (SEM) with energy dispersive spectroscopy (EDS) showed that the BOS dust consisted of very fine iron/iron oxide particles (~200-500 nm) (Longbottom *et al*. 2019a, Longbottom *et al*. 2019b). However, it was found that due to the fine particle size, it was difficult to fully resolve the smaller particles, and it was not possible to fully resolve the Zn-containing phase/particles by EDS. Similar microstructures containing these very fine particles have been reported in other BOS dust samples (Jabłońska *et al*. 2021, Stewart *et al*. 2022, Wang *et al*. 2021, Hleis *et al*. 2013) and EAF dust samples (Suetens *et al*. 2015, Sofilić *et al*. 2004, Lin *et al*. 2017).

There were also issues with the use of XRD to characterise these samples. It is well known that $Fe_3O_4$ and $ZnFe_2O_4$ have very similar lattice spacings, resulting in very similar XRD patterns (Stewart and Barron, 2020). In addition, $Fe_3O_4$ and $ZnFe_2O_4$ form a solid solution, which again is difficult to identify and quantify using XRD. For these reasons, in previous studies a single "spinel" phase was used to encompass any $Fe_3O_4$ and $ZnFe_2O_4$ or solid solution (Longbottom *et al*. 2020). Often, these issues can be overcome by substituting a longer wavelength X-ray source, which may also help overcome issues with iron fluorescence with a Cu-Kα source. However, peak broadening from the fine particle size of the BOS dust likely masks any peak shift with composition even with a longer wavelength X-rays.

The aim of the study was to overcome these difficulties in identifying the Zn-bearing phases by characterising the BOS dust using high resolution transmission electron microscopy (TEM) and Mössbauer spectroscopy. TEM microscopy was used to help with the resolving of the very fine particles in the BOS dust samples. Mössbauer spectroscopy was used to help overcome the limitations in XRD in differentiating between $Fe_3O_4$, $ZnFe_2O_4$ and their solid solution. In this study BOS dust in two conditions was studied, fresh dust collected immediately after the dewatering process, as well as self-sintered dust collected from the stockpiles at BlueScope's Port Kembla steelworks.

## EXPERIMENTAL

TEM and Mössbauer spectroscopy were used to characterise BOS dust samples. Fresh and self-sintered samples were both characterised. The fresh dust sample was collected immediately after dewatering, while the self-sintered dust was collected from the stockpiles at BlueScope's Port Kembla steelworks. The composition of the two samples, measured by XRF, is given as simple oxides in Table 1. The speciation of iron (and other phases) is not given by XRF, and was initially characterised by XRD phase analysis (see Figure 1) using Cu-kα (λ = 0.154 nm) radiation. It may be seen that iron was mainly present as wüstite and metallic Fe in the fresh BOS dust sample, with a minor amount of "magnetite". In the self-sintered sample, iron was mainly present as "magnetite" with a small amount of hematite. Iron speciation and oxidation state was further investigated as part of this study using Mössbauer spectroscopy.

TABLE 1 – XRF analyses of the BOS dust samples. The compositions are given in mass%.

| Sample | MgO | $Al_2O_3$ | $SiO_2$ | $P_2O_5$ | $SO_3$ | $K_2O$ | CaO | $TiO_2$ | MnO | $Fe_2O_3$ | ZnO |
|---|---|---|---|---|---|---|---|---|---|---|---|
| fresh | 1.8 | trace | 1.4 | trace | trace | trace | 3.2 | trace | trace | 78.2 | 13.8 |
| self-sintered | 1.5 | trace | 4.4 | trace | trace | trace | 3.9 | trace | trace | 79.8 | 8.0 |

## TEM Characterisation

TEM characterisation was carried out using an aberration corrected JEOL ARM200F equipped with an 80 $mm^2$ JEOL Centurio SDD EDS detector. The TEM was equipped with bright field and secondary electron scanning TEM detectors. Each detector measures different characteristics of the samples:

- **Bright field**: image from transmitted beam, related to sample thickness and density.
- **Secondary electron**: equivalent to SEM images, information about surface of particles.

Sample preparation of the fresh BOS dust for TEM was carried out by suspending the sample in ethanol, with the resulting suspension then held for 5 minutes in an ultrasonic cleaner to break up clumps. This suspension was then diluted further with more ethanol, which was then drawn into a transfer pipette. Two drops of the suspension were then placed onto a lacy carbon grid.

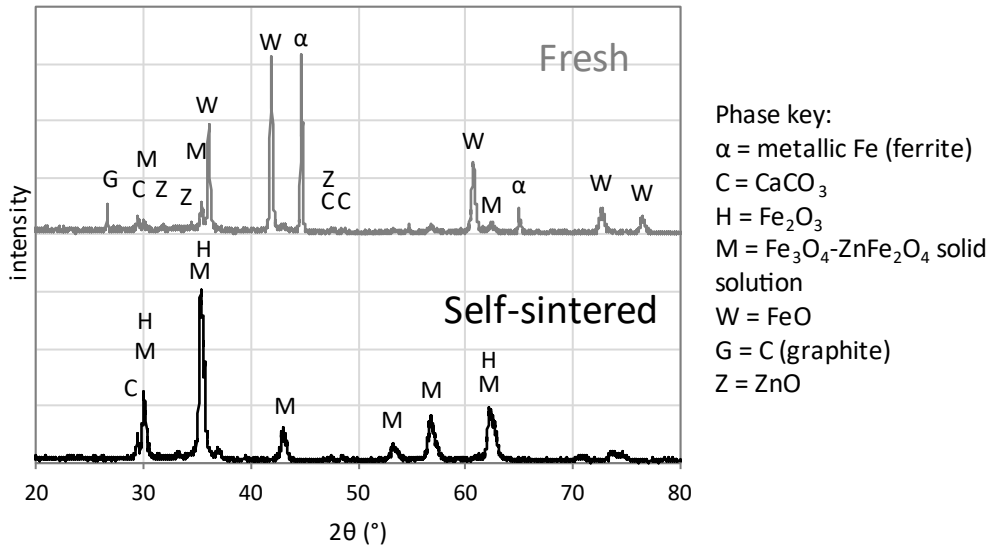


FIG 1 – XRD phase analysis of the BOS dust samples. XRD carried out using Cu-kα radiation (λ = 0.154 nm) at 1 KW power.

A ~20 g sample of the self-sintered BOS dust sample for the TEM was ground in a ring grinder for 30 s to a fine particle size so that the particles would be electron transparent. This powder was then prepared for TEM in a similar manner to that for the fresh BOS dust.

## Mössbauer characterisation

$^{57}$Fe Mössbauer spectra were obtained at room temperature using the standard transmission mode. A $^{57}$Co isotope on a Rh foil ($^{57}$CoRh) was used as the γ-ray source. The velocity scale was calibrated using a 6 μm thick α-Fe foil, and all isomer shifts are quoted relative to the α-Fe calibration at source velocity (V) values of 4 and 12 mm/s. The calibration gave a Doppler velocity amplitude of 11.4885 mm/s for the nominal V = 12 mm/s setting, and 3.8942 mm/s for the nominal V = 4 mm/s setting.

The collected spectra were fitted using the NORMOS software to allow identification of the phases. The sum of expected spectra from different phases were fitted to the measured values. Quantification of the fits to the Mössbauer spectra was conducted without standards. As such, caution should be used when considering the absolute values.

## RESULTS

To gain a better understanding of the Zn-bearing phases in BOS dust, fresh and self-sintered samples were characterised by TEM and Mössbauer spectroscopy. As both techniques use small samples (especially in the case of TEM), concerns about sample representation mean that the results (especially with quantification) should be taken as indicative rather than absolute.

## Fresh BOS dust

Bright field and secondary electron images of the fresh BOS dust sample are shown in Figure 2. EDS elemental mapping (Figure 3) was used to identify the elements present within the sample, and high magnification images of the lattice fringes (Figure 4) within the sample were used to measure lattice spacing and to aid identification of phases.

Clumps of particles were observed attached to the carbon grid. Iron was found to be present predominantly as an oxide, but with some metallic particles. The Fe-rich particles were small, with a

typical particle size being in the range 200-500 nm. This matches well with the previously reported SEM results (Longbottom *et al*. 2019b).

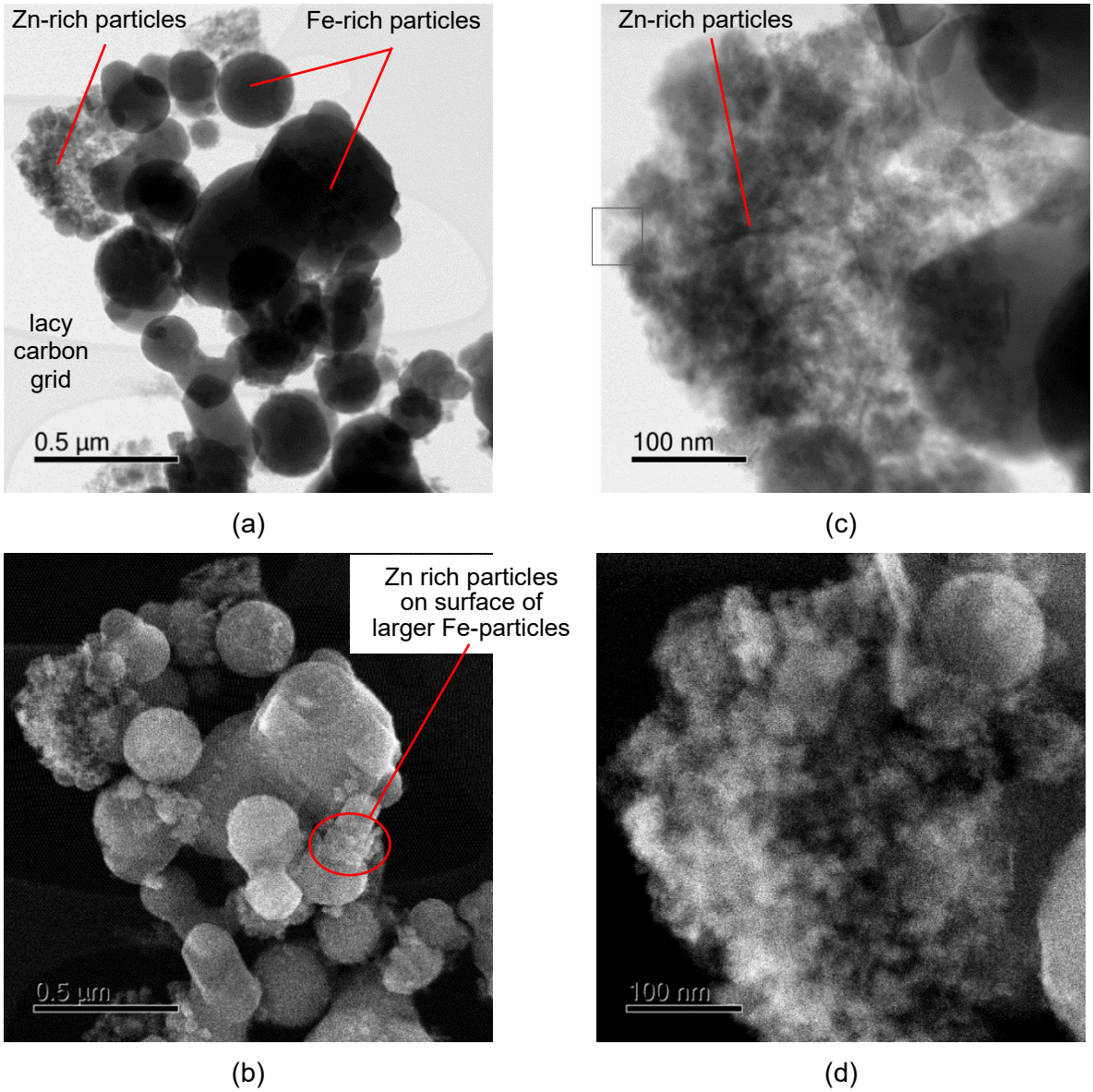


FIG 2 –TEM micrographs of fresh BOS dust. Lower magnification images: (a) bright field; and (b) secondary electron. Higher magnification images: (c) bright field; and (d) secondary electron.

Zn was mostly found present as extremely fine separate particles, attached to the iron particles. As these particles were extremely small and clustered together, it is difficult to be definitive about the particle size, even from the high magnification TEM images (Figures 2 and 3). Many of the particles appear to be < 10 nm in size. These Zn-rich particles were typically much smaller than the Fe-rich particles to which they were attached. In some cases (see Figure 3), the very small Zn-rich particles were found as a layer around metallic Fe particles. However, this behaviour was uncommon, even within the small number of clumps examined, where Zn-rich particles were more often found as clumps of Zn-rich particles attached to both metallic and oxide particles.

Examining the lattice fringes in Figure 4, crystallographic spacing (d-spacing) between the lattice planes was measured (Table 2). Comparing the measured values with the reported values for metallic Zn and ZnO (also given in Table 2), it appears that there is a strong match for hexagonal ZnO, with the measured and published d-spacings matching well. It is possible that there is a limited amount of metallic Zn in the material, with a reasonable match for the (002) reflection for metallic Zn.

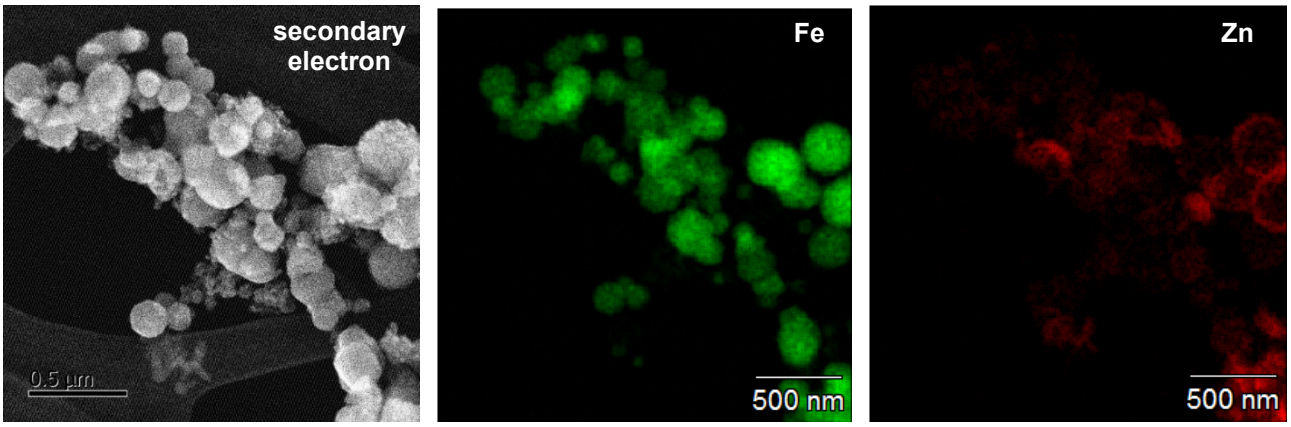


(a) (b) (c)

FIG 3 – TEM EDS elemental mapping of a fresh BOS dust sample. (a) Secondary electron image; (b) Fe elemental map; and (c) Zn elemental map.

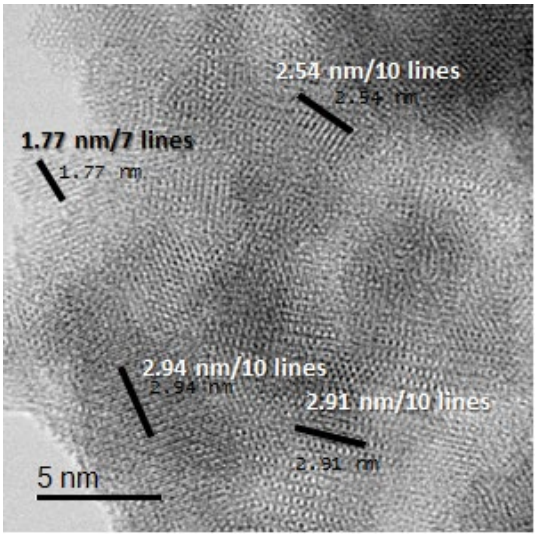


FIG 4 – High magnification bright field TEM image of fresh BOS dust (for the region shown by the rectangle in Figure 2(b)) showing lattice fringes.

TABLE 2 – Measured d-spacings from lattice fringes (Figure 4) and Published d-spacings for metallic Zn and ZnO (Crystallography Open Database, 2020).

| **average measured d-spacing** | **metallic Zn (hexagonal)** | | **ZnO (hexagonal)** | |
|---|---|---|---|---|
| (nm) | reflection plane lattice indices | d-spacing (nm) | reflection plane lattice indices | d-spacing (nm) |
| 0.293 | (002) | 0.247 | (100) | 0.290 |
| 0.253 | (100) | 0.231 | (002) | 0.261 |
| – | (101) | 0.169 | (101) | 0.254 |

Mössbauer spectroscopy results of fresh BOS dust, along with the fitted spectra for metallic iron, wüstite and $ZnFe_2O_4$ are shown in Figure 5. The spectrum of the BOS dust was fitted reasonably well with a non-magnetite, quadrupole-split doublet (likely corresponding to wüstite) between 0-2 mm/s, and a magnetite sextet (likely corresponding to metallic iron) spreading out to larger velocity scale values. A third unrestricted non-magnetic phase likely corresponded to $ZnFe_2O_4$. This analysis only considered the iron bearing phases, as only Fe nuclei are detected by Mössbauer spectroscopy using a $^{57}$CoRh γ-ray source.

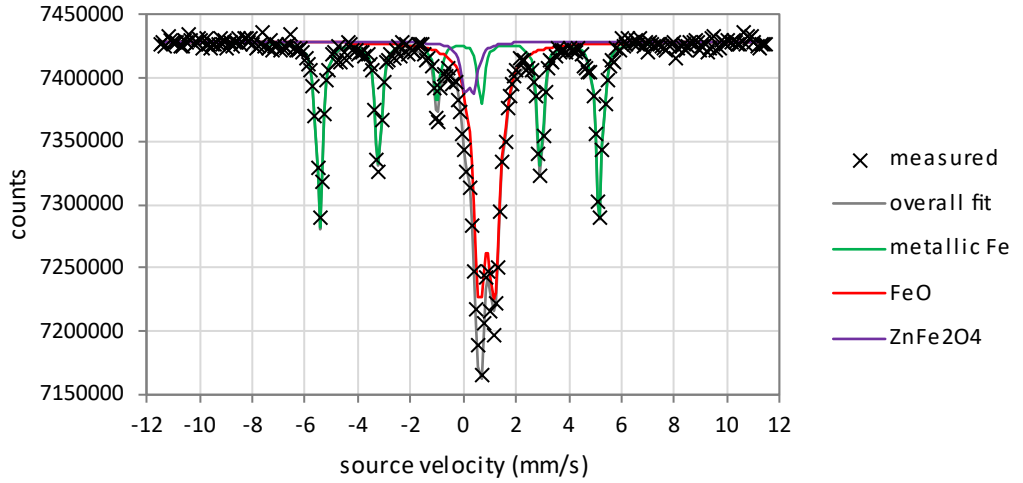


FIG 5 – Mössbauer spectra of fresh BOS dust showing the fitted spectra for metallic Fe, FeO and $ZnFe_2O_4$.

## Self-sintered BOS dust

TEM images of a self-sintered BOS dust sample are shown in Figure 6, while EDS elemental maps are shown in Figures 7. Clumps of particles were found attached to the carbon grid (Figure 6). The particles in these clumps were of varying sizes, with relatively few larger particles (> 1 μm), with more particles being in the 100-500 nm range. It should be noted that these samples were ground to ensure electron transparency, therefore both the clumps and particle size distributions are artefacts of sample preparation. While there were some very fine particles (< 50 nm) attached to the clumps, they appeared quite different to those seen in the fresh BOS dust (Figure 2). At high magnifications (Figure 6) these particles appeared to be strongly crystalline. EDS mapping (Figure 7) showed that most of the particles appear uniform in their Fe and Zn levels, indicating that the particles are likely a $Fe_3O_4$-$ZnFe_2O_4$ spinel solution.

The Mössbauer spectrum for the self-sintered BOS dust is given in Figure 8. This spectrum consisted of a broad magnetic sextet and a non-magnetic doublet. The broad magnetic sextets likely correspond to hematite (major proportion), magnetite (minor proportion) and a third iron oxide component that is likely to be Zn-substituted magnetite (i.e. the $Fe_3O_4$-rich end of the $Fe_3O_4$-$ZnFe_2O_4$ solid solution) or possibly hydrated iron oxides (such as goethite or feroxyhyte, both FeO(OH)). The non-magnetic doublet closely matches $ZnFe_2O_4$. The phases present indicate that the self-sintered dust is oxidised in comparison to the fresh sample, consistent with previously reported work (Longbottom *et al.* 2019a, 2019b 2020). The broadness of the troughs in the sextet may indicate that these phases may have been heavily substituted (most likely with Zn, which would be consistent with the presence of the $Fe_3O_4$-$ZnFe_2O_4$ solid solution) or were poorly crystalline (Cadogan, November 2020, personal communication).

## DISCUSSION

Steel plant by-products such as these BOS dust samples are not commonly examined using these techniques, often considered to be too “dirty” (e.g. containing possible volatile components) to be characterised under high vacuum. However, by extensive characterisation of these materials using more routine techniques, such as XRD, XRF, optical microscopy and SEM, these concerns can be allayed.

It should be noted that there are some limitations to the techniques used. The main issue with both the TEM and Mössbauer characterisation was with the small sample size and whether or not the sample is representative of the bulk material. For this study, there was already a comprehensive characterisation of the bulk material (Longbottom *et al*. 2019a, 2019b, 2020). With this being the case, sample representation was less of an issue. The emphasis of this study was on addressing specific issues with the pre-existing analysis around the Zn-bearing phases. The very fine particulate nature of the fresh BOS dust was identified by SEM (Longbottom *et al*. 2029b), but it was not possible to fully resolve the sample with respect to particle size.

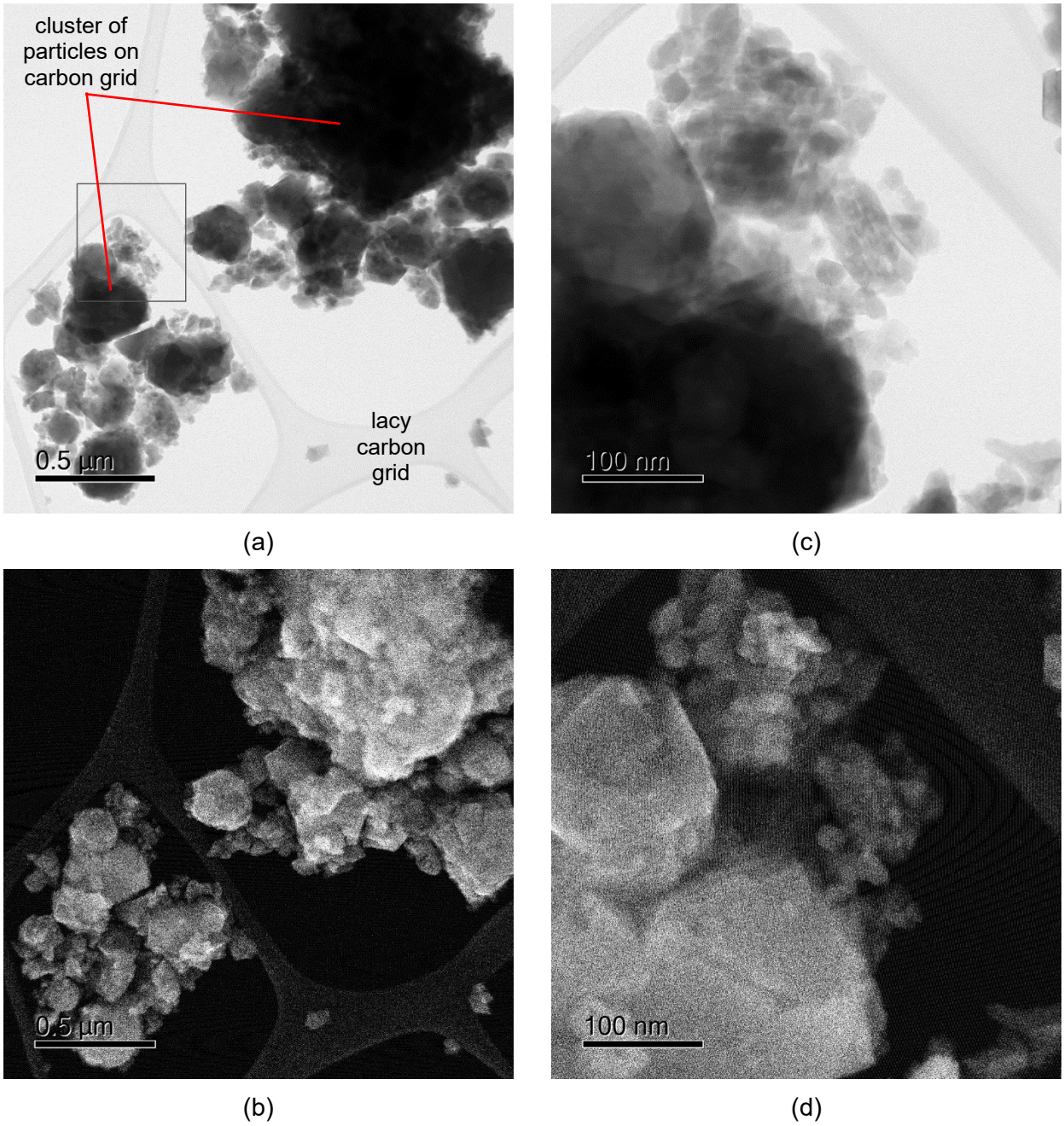


FIG 6 –TEM micrographs of self-sintered BOS dust. Lower magnification images: (a) bright field; and (b) secondary electron. Higher magnification images: (c) bright field; and (d) secondary electron.

This indicated a higher resolution technique, such as TEM was required. The detailed existing characterisation and understanding of the BOS dust samples, using XRD, SEM-EDS and XRF, allowed the use of TEM and Mössbauer spectroscopy in this study without having to characterise many samples.

Mössbauer spectroscopy used in this study was only able to characterise iron bearing phases due to the γ-ray source ($^{57}Co$) used. This means that the presence of ZnO could not be tested using this technique. While Zn is Mössbauer active, it is not commonly analysed in this way. $ZnFe_2O_4$ could be identified through its iron component.

The results also indicate that Mössbauer spectroscopy has general applicability in characterisation of metallurgical samples. While Mössbauer spectroscopy is not routinely used in slags, it would be a useful tool, aiding identification of Fe-bearing phases, or using the appropriate radiation source, phases containing any Mössbauer active elements.

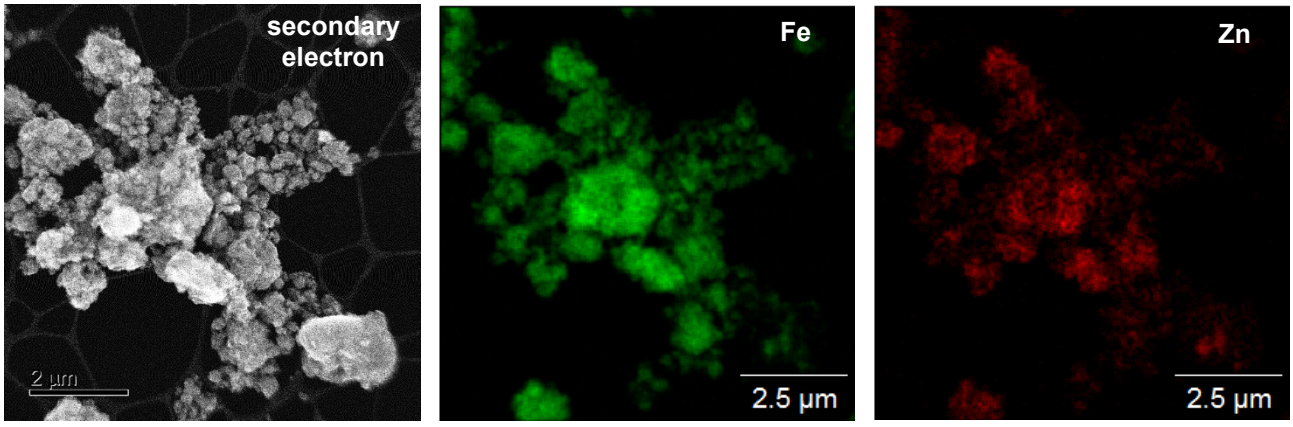


(a) (b) (c)

FIG 7 – TEM EDS elemental mapping of a self-sintered BOS dust sample. (a) Secondary electron image; (b) Fe elemental map; and (c) Zn elemental map.

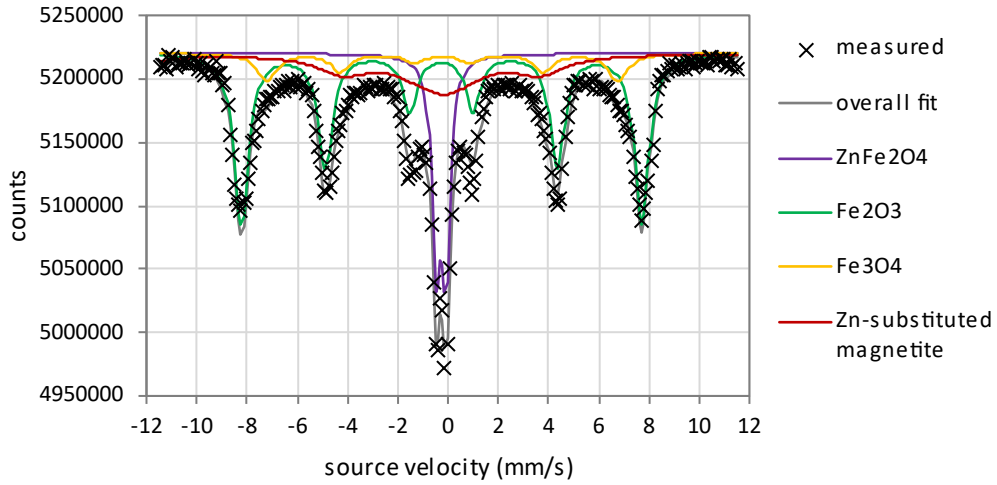


FIG 8 – Mössbauer spectra of self-sintered BOS dust showing the fitted spectra for $ZnFe_2O_4$, Fe2O3, Fe3O4 and Zn-substituted magnetite.

Further, slags are almost always characterised at room temperature, often by XRF and/or XRD. The ability of Mössbauer spectroscopy to identify components and associations in less crystalline or amorphous phases, such as glass in quenched slags, offers opportunities to improve the characterisation of these phases within slags, not possible using XRD. When used in conjunction with other techniques (XRD, XRF, SEM-EDS or WDS), Mössbauer spectroscopy will allow a fuller understanding of the slag and the phases that it contains.

The focus of this characterisation of the BOS dust was to better identify the Zn-bearing phases and their form or morphology. There were a few possible Zn-bearing phases in the BOS dust that were examined. These included metallic Zn, ZnO and $ZnFe_2O_4$. The TEM and Mössbauer characterisation given here, in conjunction with existing XRD, XRF and SEM-EDS characterisation (Longbottom *et al*. 2019a, 2019b), have allowed identification of whether these Zn-bearing phases were present in the BOS dust samples.

## Zn

There was little evidence of metallic Zn in either the fresh or self-sintered BOS dust samples. In the fresh BOS dust samples, there is a possibility that the d-spacing measured from the lattice fringes (Table 2) may match that for metallic Zn. However, this measured d-spacing was a better match for ZnO, especially when considered with the other measured d-spacing values (Table 2). Hence, it is unlikely that metallic Zn was present in either the fresh or self-sintered BOS dust samples.

## ZnO

The fresh BOS dust samples most likely contained ZnO, as very fine particles surrounding the slightly larger Fe-rich particles, as shown in Figure 2.

One of the motivations for this study was due to a discrepancy between the amount of Zn in the fresh BOS dust (identified through XRF, Table 1) and the amount of Zn that would be contained in the phases identified through XRD, as shown in Figure 1 and in Longbottom *et al*. (2020). The results from the TEM characterisation (Figure 2) give a plausible cause for this discrepancy. While a small amount of ZnO was detected by XRD (Figure 1), the TEM results showed that the ZnO particles were extremely small. Hence, it is likely that at least some of these fine particles will lead to poor diffraction patterns, and as such are likely to report to the amorphous/non-bulk crystalline fraction and unlikely to be identified as ZnO by XRD. This may also be reflected in the low intensities of the ZnO peaks for the fresh BOS dust sample in Figure 1, which may be expected to be higher with 13.8% ZnO in the sample. These very low intensities of the ZnO peaks also made estimation of the particle size from the diffraction pattern difficult.

It is unclear whether these fine ZnO particles had formed by oxidation of metallic Zn particles that had condensed during cooling of the gas, or by oxidation of Zn vapour in the gas phase. What effect these different formation mechanisms would have on the particle size and morphology of the ZnO particles is also unclear.

There was little evidence of ZnO in the self-sintered BOS dust sample.

## $ZnFe_2O_4$

In the fresh BOS dust samples, the Mössbauer spectroscopy indicated the presence of $ZnFe_2O_4$. This is consistent with the presence of a spinel phase in the XRD of the fresh BOS dust samples (Figure 1). While it was not possible to determine through XRD whether the spinel was $Fe_3O_4$, $ZnFe_2O_4$ or a solution of the two, the Mössbauer spectroscopy showed that there was some $ZnFe_2O_4$ in the fresh BOS dust sample, while not detecting $Fe_3O_4$.

In the self-sintered BOS dust sample, the major Zn-bearing phase was $ZnFe_2O_4$, most likely contained within a $Fe_3O_4$-$ZnFe_2O_4$ solid solution. Previous characterisation by XRD indicated the presence of spinel with lattice spacing close to that of both $Fe_3O_4$ and $ZnFe_2O_4$ (Figure1). This is supported by the TEM characterisation of the sample, which indicated that the sample was largely a single phase (Figure 7). The Mössbauer spectroscopy of the self-sintered sample directly identified $ZnFe_2O_4$, while also reporting the presence of magnetite with some substitution of Fe with Zn. While the Mössbauer shows the presence of both $Fe_3O_4$ and $ZnFe_2O_4$, the technique measures iron nuclei, with the response depending on the surrounding atoms in the crystal lattice (Sharma *et al*. 2013). Due to this, a single phase solid solution may be reported as two separate phases. While this seems a drawback with the Mössbauer spectroscopy, it offers a positive identification of the presence of Zn within the spinel phase. Previously this could only be speculated on from the XRD data, due to the similar lattice parameters of $Fe_3O_4$ and $ZnFe_2O_4$. Thus, it is most likely that the sample contains a $Fe_3O_4$-$ZnFe_2O_4$ solid solution with differing levels of Zn, consistent with the results from the XRD and TEM characterisation.

The improved understanding of the Zn-bearing phases within the BOS dust will allow better predictions of how it will behave during recycling. Since the Zn in the BOS dust was found to be oxidised, a reductant would be required to volatilise the Zn if extraction or separation of Zn from the dust is necessary. For recycling into the BOS vessel, the Zn-bearing phases in the fresh and self-sintered BOS dust are different, affecting how each would interact with slag. ZnO (high ZnO activity, very small particle size) in the fresh dust will interact differently with the BOS slag than the $Fe_3O_4$-$ZnFe_2O_4$ solid solution (lower ZnO activity) found in the self-sintered dust.

## Comparison with reported steel plant by-products

Other studies have characterised BOS dust samples from steel plants around the world. The current BOS dust samples contain high Zn levels in comparison to other reported compositions for BOS dust (Kelebek *et al*. 2004, Steer *et al*. 2014, Vereš *et al*. 2015, Gargul *et al*. 2016, Jabłońska *et al*. 2021, Stewart *et al*. 2022). Typically, the phases found in the BOS dust samples were a close match to those in the fresh BOS dust sample, with metallic iron, wüstite and smaller amounts of magnetite

and/or hematite. The Zn-bearing phases reported in other BOS samples are summarised in Table 3.

Several studies on BOS dust have used different techniques to identify the presence of $ZnFe_2O_4$ (Table 3). In general, $ZnFe_2O_4$ was identified, although often identified by XRD, which may result in difficulties in differentiation between $ZnFe_2O_4$ and $Fe_3O_4$ (Stewart and Barron, 2020).

TABLE 3 – Reported Zn-bearing phases in BOS dust.

| Study | Technique(s) | Majority phases | Reported Zn-bearing phases |
|---|---|---|---|
| Kelebek *et al*. (2004) | XRD, SEM | FeO, $Fe_2O_3$ | $ZnFe_2O_4$ identified by XRD, not differentiated from $Fe_3O_4$ |
| Steer *et al*. (2014) | XRD, wet sizing | not reported | ZnO |
| Vereš *et al*. (2015) | XRD, Mössbauer | metallic Fe, FeO, $Fe_3O_4$, $Fe_2O_3$ | ZnO, $ZnFe_2O_4$ |
| Gargul *et al*. (2016) | XRD | metallic Fe, FeO, $Fe_3O_4$ | ZnO |
| Jabłońska *et al*. (2021) | XRD | $Fe_3O_4$, ZnO, $ZnFe_2O_4$ | ZnO, $ZnFe_2O_4$ identified by XRD, differentiated from $Fe_3O_4$ using Rietveld fitting |
| Stewart *et al*. (2022) | Mössbauer, XRD, SEM, XRF, digestion + AAS | metallic Fe, FeO, $Fe_3O_4$, $Fe_2O_3$ | Small amount of Zn in solution in $Fe_3O_4$<br>No $ZnFe_2O_4$ identified |

Some studies used Mössbauer spectroscopy to attempt to identify $ZnFe_2O_4$, with some studies reporting $ZnFe_2O_4$ and others not (Vereš *et al*. 2015, Stewart and Barron, 2020). The variability between samples was speculated to be related to the specific dust extraction-gas cleaning systems and dust storage for each plant, with samples that contain more oxidised samples having more $ZnFe_2O_4$. These findings correspond well with the phases in the fresh and self-sintered BOS dust samples in the current study, with the more oxidised self-sintered sample containing more $ZnFe_2O_4$ than the fresh sample.

EAF dust often contains more Zn than BOS dust (Suetens *et al*. 2015, Sofilić *et al*. 2004), due to the higher proportion of scrap in the feed. As such, it is useful to consider EAF dust in comparison to the Zn-rich BOS dust samples from the current study. These Zn-rich EAF dust samples were found to contain both ZnO and $ZnFe_2O_4$. Again, these samples compare well with the BOS dust samples in the current study.

## CONCLUSIONS

Characterisation of fresh and self-sintered BOS dust by TEM and Mossbauer spectroscopy was carried out to give a better understanding of the Zn-bearing phases within the samples, to improve the understanding of how the BOS dust will behave during recycling.

In the fresh BOS dust sample, TEM showed that Zn was mostly present as extremely fine separate particles of ZnO, attached to the iron particles. These extremely fine particles were < 10 nm in size. While most of the Zn was contained within these extremely small particles, Mössbauer spectroscopy identified a small amount of $ZnFe_2O_4$ within the sample (most likely contained within a $Fe_3O_4$-$ZnFe_2O_4$ spinel solid solution).

The self-sintered BOS dust sample was significantly different. The Zn-bearing phase in this sample was a $Fe_3O_4$-$ZnFe_2O_4$ solid solution. While this phase had previously been identified by XRD, Mössbauer spectroscopy gave positive identification of Zn within the spinel phase.

The ability to positively identify the phases in complex samples such as these BOS dust indicate that these techniques should have further application in the characterisation of slag, or other metallurgical by-product materials.

## ACKNOWLEDGEMENTS

The authors acknowledge use of the facilities and the assistance of David Wexler and David Mitchell at the UOW Electron Microscopy Centre. This research used equipment funded by the Australian Research Council (ARC) Linkage, Infrastructure, Equipment and Facilities (LIEF) grant LE120100104 located at the UOW Electron Microscopy Centre. The authors thank Sean Cadogan (UNSW Canberra) for the Mössbauer analysis measurements and interpretation of results. Funding support from the Australian Research Council Industrial Transformation Research Hubs Scheme (Projects IH130100017; IH200100005) and BlueScope is gratefully acknowledged.

## REFERENCES

Ahmed, H M, Persson, A, Ökvist, L S and Björkman, B, 2015. Reduction behaviour of self-reducing blends of in-plant fines in inert atmosphere, *ISIJ International*, 55(10): 2082-2089.

Crystallography Open Database, 2020. Available from: <www.crystallography.net/cod/> [accessed 10 March 2020].

Gargul, K, Jarosz, P and Małecki, S, 2016. Alkaline Leaching of Low Zinc Content Iron-Bearing Sludges, *Arch. Metall. Mater.*, 61(1): 43-50.

Hleis, D, Fernández-Olmo, I, Ledoux, F, Kfoury, A, Courcot, L, Desmonts, T and Courcot, D, 2013. Chemical profile identification of fugitive and confined particle emissions from an integrated iron and steelmaking plant, *J. of Hazardous Materials*, (250-251): 246-255.

Jabłońska, M, Rackwał, M, Wawer, M, Kądziołka-Gaweł, M, Teper, E, Krzykawski, T and Smołka-Danielowska, D, 2021. Mineralogical and Chemical Specificity of Dusts Originating from Iron and Non-Ferrous Metallurgy in the Light of Their Magnetic Susceptibility, *Minerals*, 1(2): 216.

Kelebek, S, Yörük, S and David, B, 2004. Characterization of basic oxygen furnace dust and zinc removal by acid leaching, *Minerals Engineering*, 17: 285-291.

Lin, X, Peng, Z, Yan, J, Li, Z, Hwang, J-Y, Zhang, Y, Li, G and Jiang T, 2017. Pyrometallurgical recycling of electric arc furnace dust, *J. Cleaner Production*, 149: 1079-1100.

Longbottom, R J, Monaghan, B J, Zhang, G, Pinson, D J and Chew, S J, 2019a. Self-sintering of BOS Filter Cake for Improved Recyclability, *ISIJ International*, 59(3): 432-441.

Longbottom, R J, Monaghan, B J, Pinson, D J and Chew, S J, 2019b. Understanding the Self-Sintering Process of BOS Filter Cake for Improving Its Recyclability, *J. Sustainable Metallurgy*, 5: 429-441.

Longbottom, R J, Monaghan, B J, Pinson, D J, Webster, N A S and Chew, S J, 2020. *In situ* Phase Analysis during Self-sintering of BOS Filter Cake for Improved Recycling, *ISIJ International*, 60(11): 2436-2445.

Nyirenda, R L, 1991. The processing of steelmaking flue-dust: A review, *Minerals Engineering*, 4(7-11):1003-1025.

Sharma, V K, Klingelhofer, G and Nishida, T, 2013. Mössbauer Spectroscopy: Applications in Chemistry, Biology, and Nanotechnology, Part V Iron Oxides, pp. 349-532 (John Wiley & Sons, Hoboken, USA).

Steer, J, Grainger, C, Griffiths, A, Griffiths, M, Heinrich, T and Hopkins, A, 2014. Characterisation of BOS steelmaking dust and techniques for reducing zinc contamination, *Ironmaking and Steelmaking,* 41(1): 61-66.

Stewart, D J C and Barron, A R, 2020. Pyrometallurgical removal of zinc from basic oxygen steelmaking dust – A review of best available technology, *Resources, Conservation & Recycling*, 157: 104746.

Stewart, D J C, Scrimshire, A, Thomson, D, Bingham, P A and Barron, A R, 2022. The chemical suitability for recycling of zinc contaminated steelmaking by-product dusts: The case of the UK steel plant, *Resources, Conservation & Recycling Advances*, 14: 200073.

Suetens, T, Guo, M, Van Acker, K and Blanpain, B, 2015. Formation of the $ZnFe_2O_4$ phase in an electric arc furnace off-gas treatment system, *J. of Hazardous Materials*, (287): 180-187.

Vereš, J, Šepelák, V and Hredzák, S, 2014. Chemical, mineralogical and morphological characterisation of basic oxygen furnace dust, *Mineral Processing and Extractive Metallurgy, Transactions of the Institutions of Mining and Metallurgy: Section C*, 124(1): 1-8.

Wang, J, Zhang, Y, Cui, K, Fu, T, Gao, J, Hussain, S and AlGarni, T S, 2021. Pyrometallurgical recovery of zinc and valuable metals from electric arc furnace dust – A review, *J. Cleaner Production*, 298: 126788.